

$\mu^+ \rightarrow e^+\gamma$ search with the MEG experiment: Results and perspectives

L. GALLI on behalf of the MEG COLLABORATION

INFN, Sezione di Pisa - Pisa, Italy

(ricevuto il 29 Settembre 2011; pubblicato online il 24 Gennaio 2012)

Summary. — I present the preliminary results of the data collected by the MEG detector at the Paul Scherrer Institute in 2009 in search of the lepton flavour violating decay $\mu^+ \rightarrow e^+\gamma$ with a sample of 6×10^{13} muon decays on target.

PACS 11.30.Fs – Global symmetries (*e.g.*, baryon number, lepton number).

PACS 14.60.Ef – Muons.

PACS 13.35.Bv – Decays of muons.

1. – Introduction

In the minimal standard model (SM) the lepton flavour violating (LFV) processes are not allowed at all; leptons are grouped in separated doublets and the lepton flavour conservation is built in by hand assuming vanishing neutrino masses. Nevertheless, the neutrino oscillations are now established facts (for a continuously updated review, see [1]) and the neutrino masses are definitely not vanishing; then, LFV in the neutral sector is an experimental reality, while until now there are no corresponding indications in the charged sector. When massive neutrinos and neutrino oscillations are introduced in the SM, LFV decays of charged leptons are predicted, but at immeasurably small levels (branching fractions $\sim 10^{-50}$ with respect to SM decays). However, Supersymmetric and especially GUT supersymmetric theories (SUSY and SUSY-GUT) naturally accommodate finite neutrino masses and predict relatively large (and probably measurable) branching ratios (BR) for LFV processes (see for example [2-6]). Therefore, sizable flavour violation processes would be strong indications in favour of new physics beyond the SM.

Even if searches for charged LFV effects have, so far, yielded no results, they had a relevant impact on the particle physics development: for example, the non-observation of the $\mu^+ \rightarrow e^+\gamma$ decay [7] established that the muon and the electron are two distinct leptons [8] and the stronger and stronger constraints on this process were basic arguments for introducing a second neutrino (ν_μ) [9]. At the beginning of the third millennium, the search for charged LFV reactions allows to explore SUSY mass scales up to 1000–10000 TeV (even out of LHC reach) and to give insights about large mass range, parity violation, number of generations, etc.

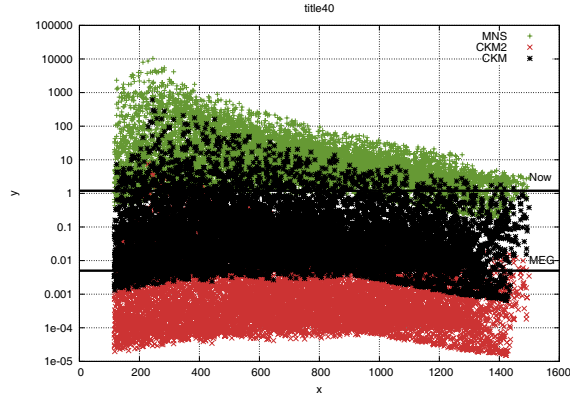


Fig. 1. – Branching ratio of $\mu^+ \rightarrow e^+\gamma$ decay (in units of 10^{-11}) as a function of $M_{1/2}$ (GeV) for three classes of SUSY models [5]. The horizontal line labelled “Now” is the present experimental limit: $BR(\mu^+ \rightarrow e^+\gamma) \leq 1.2 \times 10^{-11}$ [11].

Figure 1 illustrates examples of recent theoretical predictions for charged LFV processes in the SUSY frame: the $\mu^+ \rightarrow e^+\gamma$ BR is shown as a function of $M_{1/2}$ (in GeV) for three different classes of models [5]. A detailed review of the mechanisms which might induce LFV processes and of the relation between LFV and other signs of new physics (like Muon Anomalous Magnetic Moment) can be found in [10].

Many experiments are under way or in preparation which would test the theoretical predictions with unprecedented levels of sensitivity in the μ and in the τ channels.

Note that not only positive results, but also negative results could be very significant, since they would tightly constrain the multi-dimensional SUSY parameter space. We also stress that searching for LFV processes in different channels and with different leptons is one of the most powerful tools to discriminate between different models. Figure 2 shows the improvement with time of the upper limits for some LFV processes. In this paper I present the search for $\mu^+ \rightarrow e^+\gamma$ decay performed by the MEG collaboration.

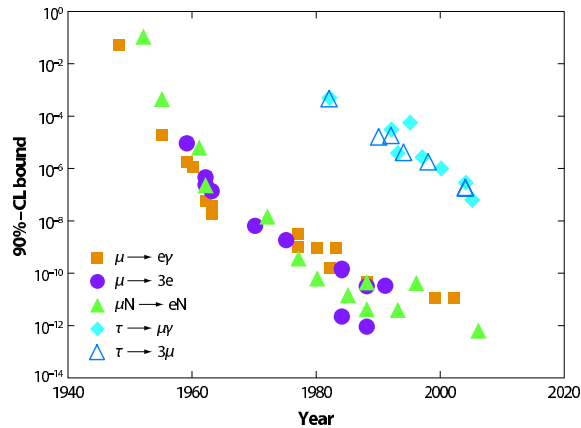


Fig. 2. – Improvement with time of some LFV searches (from [10]).

TABLE I. – The performances of previous $\mu \rightarrow e\gamma$ experiments compared with that expected for MEG. All the quoted resolutions are FWHM. The asterisk shows an average of the numbers given in [11].

Place	Year	$\Delta E_e/E_e$	$\Delta E_\gamma/E_\gamma$	$\Delta t_{e\gamma}$	$\Delta\theta_{e\gamma}$	Upper limit	Refs.
SIN	1977	8.7%	9.3%	1.4 ns	–	$< 1.0 \times 10^{-9}$	[13]
TRIUMF	1977	10%	8.7%	6.7 ns	–	$< 3.6 \times 10^{-9}$	[14]
LANL	1979	8.8%	8%	1.9 ns	37 mrad	$< 1.7 \times 10^{-10}$	[15]
LANL	1986	8%	8%	1.8 ns	87 mrad	$< 4.9 \times 10^{-11}$	[16]
LANL	1999	1.2%*	4.5%*	1.6 ns	17 mrad	$< 1.2 \times 10^{-11}$	[11]
PSI	≈ 2013	0.8%	4.0%	0.15 ns	19 mrad	$< 1 \times 10^{-13}$	MEG

2. – Signal and background

The $\mu \rightarrow e\gamma$ decay is the historical channel where charged LFV is searched for. Positive muons (selected to avoid nuclear captures in the stopping target), coming from decay of π^+ produced in proton interactions on fixed target, are brought to stop and decay at rest, emitting simultaneously a γ and a e^+ in back-to-back directions. Since the e^+ mass is negligible, both particles carry away the same kinetic energy: $E_{e^+} = E_\gamma = m_\mu/2 = 52.83$ MeV. The signature is very simple, but, because of the finite experimental resolution, it can be mimed by two types of background:

- a) The *physical* or *correlated* background, due to the radiative muon decay (RMD): $\mu^+ \rightarrow e^+\bar{\nu}_\mu\nu_e\gamma$. The *BR* of RMD process is $(1.4 \pm 0.2)\%$ of that of usual muon Michel decay $\mu^+ \rightarrow e^+\bar{\nu}_\mu\nu_e$ for $E_\gamma > 10$ MeV.
- b) The *accidental* or *uncorrelated* background, due to the coincidence, within the analysis window, of a e^+ coming from the usual muon decay and a γ coming from RMD, $e^+ - e^-$ annihilation in flight, e^+ bremsstrahlung in a nuclear field, etc.

While signal and RMD rates are proportional to the muon stopping rate R_μ , the accidental background rate is proportional to R_μ^2 , since both particles come from the beam; the accidental background is dominant and sets the limiting sensitivity of a $\mu \rightarrow e\gamma$ experiment. Then, in the search for $\mu^+ \rightarrow e^+\gamma$ decay a continuous muon beam is preferred and R_μ must be carefully chosen to optimize the signal-to-noise ratio. The number of background events depends on the sizes of the signal region, which are determined by the experimental resolutions. Physical effects which degrade the resolution, as multiple scattering and energy loss, are reduced by using “surface” muons, *i.e.* muons produced by pions stopped very close to the surface of π production target, which are efficiently brought to rest in thin targets. Moreover, high resolution detectors are mandatory. table I shows the figures of merit obtained by previous $\mu \rightarrow e\gamma$ experiments compared with the final goals of the MEG [12] experiment; the 90% C.L. upper limits on $\mu \rightarrow e\gamma$ *BR* are also reported.

3. – Detector and calibration systems

The MEG experiment [12] (fig. 3) uses the secondary $\pi E5$ muon beam line extracted from the PSI (Paul Scherrer Institute) proton cyclotron, the most powerful continuous

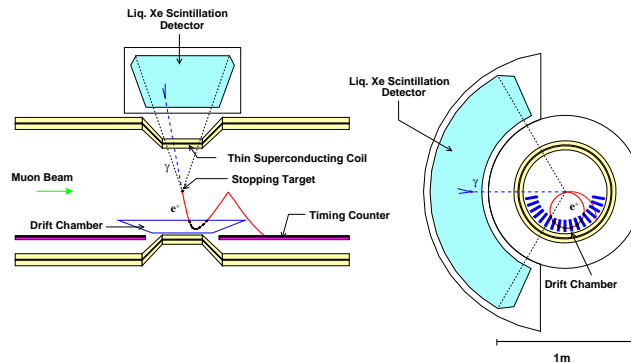


Fig. 3. – Layout of the MEG experiment.

hadronic machine in the world (maximum proton current $I = 2.2$ mA). A $3 \times 10^7 \mu^+$ /s beam is stopped in a $205 \mu\text{m}$ slanted polyethylene target. The e^+ momentum is measured by a magnetic spectrometer, composed by an almost solenoidal magnet (COBRA) with an axial gradient field and by a system of sixteen ultra-thin drift chambers (DC). The e^+ timing is measured by two double-layer arrays of plastic scintillators (Timing Counter, from now on: TC): the external layer is equipped with two sections of 15 scintillating bars each, the internal one with 512 scintillating read by APDs fibers to measure the transverse positron impact coordinate on the scintillating bars. The γ energy, direction and timing are measured in a ≈ 800 l volume liquid xenon (LXe) scintillation detector. The LXe as scintillating medium was chosen because of its large light yield (comparable with that of NaI) in the VUV region ($\lambda \approx 178$ nm), its homogeneity and the fast decay time of its scintillation light (≈ 45 ns for γ 's and ≈ 22 ns for α 's) [17]. The LXe volume is viewed by 846 Hamamatsu 2" PMTs, specially produced to be sensitive to UV light and to operate at cryogenic temperatures. Possible water or oxygen impurities in LXe are removed by circulating the liquid through a purification system.

A FPGA-FADC based digital trigger system was specifically developed to perform a fast estimate of the γ energy, timing and direction and of the positron timing and direction; the whole information is then combined to select events which exhibit some similarity with the $\mu \rightarrow e\gamma$ decay. The signals coming from all detectors are digitally processed by a 2 GHz custom made waveform digitizer system to identify and separate pile-up hits.

Several calibration tools (LEDs, point-like α sources deposited on wires [18], Am-Be sources, Michel decays, through going cosmic μ 's, a neutron generator, 55 MeV and 83 MeV γ 's from charge exchange reaction $\pi^-p \rightarrow \pi^0n$, γ -lines from nuclear reactions induced by a CW accelerator, etc.) are frequently used to measure and optimize the detector performances and to monitor their time stability. The experimental resolutions measured in summer of 2010 (the time of this conference) were: $\sigma_p/p = 0.75\%$, $\sigma_\phi = 8$ mrad and $\sigma_\theta = 11$ mrad for e^+ 's, $\sigma_E/E = 2.1\%$ and $\sigma_x = 5.5$ mm for γ 's and $\sigma_{\Delta T} = 142$ ps for $e^+ - \gamma$ relative timing. Significant improvements are expected in the following years, which should make these numbers closer to the table I goals.

A new calibration method for the tracking system is also operative from the 2010, it takes advantage from the elastic Mott scattering of monochromatic positrons into a dedicated polyethylene target. These events can be used to measure the tracker momentum

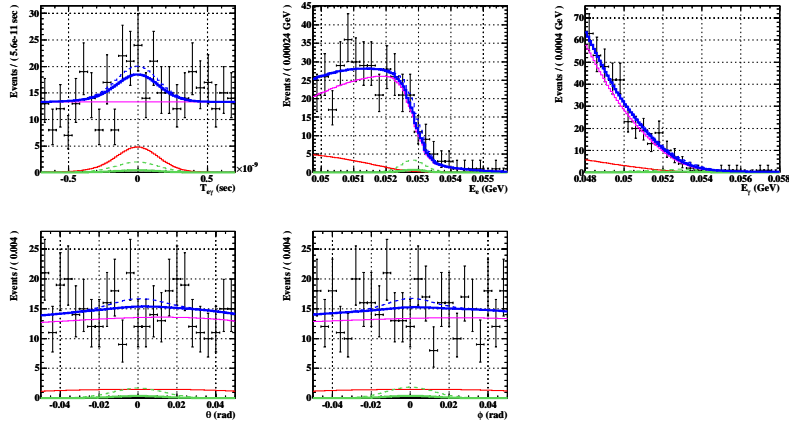


Fig. 4. – (Colour on-line) Results of MEG maximum likelihood analysis. From top to bottom, from left to right: $\Delta T_{e\gamma}$, E_{e^+} , E_γ , $\theta_{e\gamma}$, $\phi_{e\gamma}$. Signal PDFs are in green, RMD PDFs in red, accidental background PDFs in magenta and total PDFs in blue. The black dots represent the experimental data and the dashed lines the 90% C.L. upper limit on the number of signal events.

resolution at the signal energy and investigate systematic uncertainties in the positron track reconstruction.

4. – Data analysis and preliminary result

The data are analysed with a combination of blind and likelihood strategy. Events are pre-selected on the basis of loose cuts, requiring the presence of a track and $|\Delta T_{e\gamma}| < 4$ ns. Preselected data are processed several times with improving calibrations and algorithms and events falling within a tight window (“blinding box”, BB) in the $(E_\gamma, \Delta T_{e\gamma})$ -plane are hidden. The remaining pre-selected events fall in “sideband” regions and are used to optimize the analysis parameters, study the background and evaluate the experimental sensitivity under the zero signal hypothesis. When the optimisation procedure is completed, the BB is opened and a maximum likelihood fit is performed to the distributions of five kinematical variables (E_{e^+} , E_γ , $\Delta T_{e\gamma}$, $\theta_{e\gamma}$ and $\phi_{e\gamma}$), in order to extract the number of Signal (S), RMD (R) and Accidental Background (B) events. Probability Distribution Functions (PDFs) are determined by using calibration measurements and MC simulations for S , theoretical formulae folded with experimental resolution for R ⁽¹⁾ and sideband events for B . Michel positrons are used to calculate the normalization factor needed to convert an upper limit on S into an upper limit on $BR(\mu^+ \rightarrow e^+\gamma)$. The analysis procedure was applied for the first time to the data collected in 2008, with reduced statistics and not optimal apparatus performances, and a first result was published [19]: $BR(\mu \rightarrow e\gamma) \leq 2.8 \times 10^{-11}$ at 90% C.L., about twice worse than the present bound [11]. In 2009 a larger and better quality data sample was collected and the analysis procedure was repeated. 370 events fell in the BB, defined as $48 \text{ MeV} < E_\gamma < 58 \text{ MeV}$ and $|\Delta T_{e+\gamma}| < 0.7$ ns. Figure 4 shows the results of the maximum likelihood fit to the five

⁽¹⁾ In RMD events, the kinematical boundaries introduce a correlation between E_{e^+} , E_γ and positron-gamma relative angle which must be taken into account in the PDF.

kinematical variables for 2009 data. The (preliminary!) best fit result was $S = 3.0$ and $R = 35$. The analysis was repeated by different groups varying the approach (frequentistic and Bayesian), the handling of sideband information and the estimated numbers of R and B in the BB; the best fit value for S ranged between 3 and 4.5 and the corresponding 90% C.L. interval was (0, 15); then, a (preliminary!) 90% C.L. upper limit was set: $BR(\mu \rightarrow e\gamma) \leq 1.5 \times 10^{-11}$, close to the current experimental limit.

5. – Perspectives and conclusions

The MEG collaboration has already performed a new data collection campaign in 2010, collecting a sample twice that of 2009 in comparable running condition and detector performances. The analysis is significantly improved, in particular in the positron reconstruction and the related systematics reduced. A new result with 2009 and 2010 data together is going to be obtained within this summer.

The experiment is expected to run at least until the end of 2012; this will produce a huge increase in statistics and, taking into account further improvements of detector performances, will allow to reach a sensitivity $\sim 5 \times 10^{-13}$, (30–50) times better than the present upper bound.

* * *

I am grateful to the many MEG colleagues who helped me in the preparation of the talk and of these proceedings. A special thank to the Conference Organizers that invited me to present MEG and to enjoy the beautiful slopes of La Thuile.

REFERENCES

- [1] STRUMIA A. and VISSANI F., *Neutrino masses and mixings and ...*, Preprint hep-ph/0606054 (2006).
- [2] BARBIERI R. and HALL L. J., *Phys. Lett. B*, **338** (1994) 212.
- [3] BARBIERI R., HALL L. J. and STRUMIA A., *Nucl. Phys. B*, **445** (1995) 219.
- [4] HISANO J. *et al.*, *Phys. Lett. B*, **391** (1997) 341; *Phys. Lett. B*, **391** (1997) 357(E).
- [5] CABIBBI L. *et al.*, *Phys. Rev. D*, **74** (2006) 116002.
- [6] CABIBBI L. *et al.*, *Proceedings of the Europhysics Conference on High Energy Physics: HEP2009 (Cracow)* (2009) p. 167.
- [7] HINCKS E. P. and PONTECORVO B., *Phys. Rev.*, **73** (1948) 257.
- [8] LOKANATHAN S. and STEINBERGER J., *Phys. Rev. A*, **98** (1955) 240.
- [9] FEINBERG G., *Phys. Rev.*, **110** (1958) 1482.
- [10] MARCIANO W. J., MORI T. and RONEY J. M., *Annu. Rev. Nucl. Part. Sci.*, **58** (2008) 315.
- [11] AHMED M. *et al.* (MEGA COLLABORATION), *Phys. Rev. D*, **65** (2002) 112002.
- [12] BALDINI A. *et al.* (MEG COLLABORATION), Proposal to INFN, see <http://meg.psi.ch> (2002).
- [13] VAN DER SCHAAF A. *et al.*, *Nucl. Phys. A*, **340** (1980) 249.
- [14] DEPOMMIER P. *et al.*, *Phys. Rev. Lett.*, **39** (1977) 113.
- [15] KINNISON W. W. *et al.*, *Phys. Rev. D*, **25** (1982) 2846.
- [16] BOLTON R. D. *et al.*, *Phys. Rev. D*, **38** (1988) 2077.
- [17] BALDINI A. *et al.*, *Nucl. Instrum. Methods A*, **545** (2005) 753.
- [18] BALDINI A. *et al.*, *Nucl. Instrum. Methods A*, **565** (2006) 589.
- [19] MEG COLLABORATION, *Nucl. Phys. B*, **834** (2010) 1.